AUTOMATED SEGMENTATION OF HIP CARTILAGES IN MULTI-SLICE MR DATA

M. Khanmohammadi [1*], R. A. Zoroofi [2*], Y. Sato [3Θ], T. Nishii[¤], K. Nakanishi[¤], H. Tanaka[¤], N. Sugano[¤], H. Yoshikawa[¤], H. Nakamura[†], S. Tamura [Θ]

[*] Control and Intelligent Processing Center of Excellence
Electrical and Computer Engineering Department
Faculty of Engineering, University of Tehran, Tehran, IRAN.
[Θ] Division of Image Analysis
[¤]Department of Orthopaedic Surgery
[†]Department of Radiology
Osaka University Graduate School of Medicine, Osaka , JAPAN.
Email: [1]m.khanmohamadi@ece.ut.ac.ir [2] zoroofi@ut.ac.ir [3] yohsi@image.med.osaka-u.ac.jp

Abstract- **Segmentation of the hip cartilages is clinically important. Automatic segmentation of the hip bones is the first step in segmenting the cartilages as they are stiffer and less probable to be damaged in diseases. In this study, we propose an automatic multi step technique for segmentation the femoral head and acetabulum using clinically obtained multi-slice T1-weighted MR data through the following steps: 1) We resample data sets with a modified Sinc interpolation technique To perform an isotropic dataset, 2) By assuming a spherical shape for the femur, we estimate the center of the femoral head by a Hough transform,3) We develop a multistage approach for bone segmentation that employs a modified self-adaptive on-line vector quantization technique for a low-level image classification and utilizes a region-growing strategy for a high-level feature extraction, 4) We localize the hip joint space edges by customizing the anatomical constraint, 5) Finally, from our recent research we use segmented articular space to segment the acetabular and femoral head cartilages from each other. The techniques are implemented in C++ and Matlab programming languages. The feasibility of the proposed techniques is successfully evaluated in the presence of 40 hips including 1200 MR images.**

Keywords **- Hough Transform; Directional Derivative Filter; Cartilage Segmentation; Adaptive Thresholding; Vector Quantization.**

I. INTRODUCTION

Hip joint has a main role in human locomotion and bearing the body weight. The common causes of hip joint are osteoarthritis and dysplasia [1]. Quantitative evaluation of cartilage is a great help for orthopedists to study the pathogenesis of joint dysfunction. The thickness of the cartilage is only a few millimeters, so accurate segmentation is important for corresponding quantifications [2].

MR imaging is preferred for cartilage imaging because of its noninvasiveness, high soft-tissue contrast ability, and its multi-planar and three-dimensional data acquisition [2], [3]. A normal hip joint is formed like a ball and socket shape. The femoral head is located in the acetabulum, in the pelvic bone. The head of the femur is reinforced in its position by very powerful ligament. The surfaces of femoral head and acetabulum are covered by cartilages. The articular space separate these two cartilages that can be appeared after continues leg traction [4].

The purpose of this study is to develop an automatic technique to segment the hip joint cartilages from multi slice MR data acquired by T1-weighted 3D fast spoiled gradient echo (SPGR). As the goal of hip cartilage segmentation and because of the bone stiffness we need to segment the femoral head and acetabular bone accurately. Thus, we apply a vector quantization algorithm to segment the bones. The hip joint space is finally segmented by labeling the obtained edges and imposing the anatomical constraint associated with the location of the cartilages and femoral head center in the hip joint. With using the segmented articular space localized in our previous work [6] we can segment the hip joint cartilages from each other.

In Section II, we explain the acquired data sets and the proposed techniques. In Section III, we evaluate the performance of the developed techniques in the presence of the available data sets; while in our previous work we did not quantify the method. The paper ends with the concluding remarks mentioned in Section IV.

II. METHODOLOGY

Data Set

MR imaging is performed with fat-suppressed 3D fast spoiled gradient echo (SPGR) sequence using a unilateral surface coil on a 1.5-T MR system [1]. In a typical MR data set of a hip joint, acetabular and femoral cartilages are attached to each other. To allow clear separation of acetabular and femoral cartilage on MR images, the original continuous leg traction technique is used during MR imaging [4]. The voxel dimensions of the MR data in our study were non-cubic. We up-sample the data in the sagittal direction by Sinc interpolation, i.e., zero expansion in the frequency domain to reduce the effect of unwanted Gibbs ringing. The resultant volume data contains 256x256x192 voxels.

Proposed Technique

The proposed technique is a multi-step algorithm for accurate segmentation of the hip joint cartilages. The steps are as follows.

A. Femur Center Estimation

The femoral head typically has a spherical shape with radius of around 20 to 25 mm. in our previous work, the center of the sphere approximated femoral head was estimated, by embedding this constraint into the mechanism of the Hough transform [6]. By employing the estimated femoral head center and imposing the anatomical information about the size of the femoral head, the region of interest (ROI) is automatically selected. Fig 1 shows a typical example

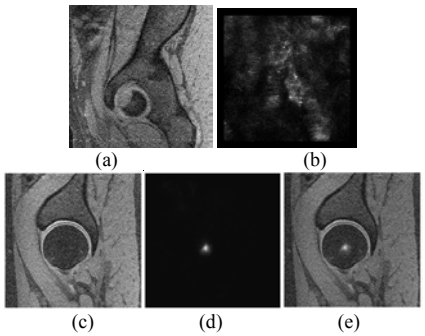

Fig1: Automatic estimation of the femoral head center. (a) Shows a typical slice far from the femoral head center. (b) Illustrates the Hough space associated with 1(a), (c) Shows a typical slice near the femoral head center. (d) Illustrates the Hough space associated with 1(c), (e) Overlaid of 1(c) with 1(d).

of finding the femoral head center and choosing the ROI.

B. Bone segmentation

Articular cartilage is surrounded by acetabulum and femoral head bone [4]. As the reason of bone stiffness in comparison with cartilage, it damages less in the joint disease [1]. Thus, the first step of segmenting the hip joint cartilages is to segment the acetabular and femoral head bones. In our previous work for bone segmentation we customized Otsu adaptive thresholding [7] and 3D morphological operations [3]. However, in some of the slices of the data sets it did not work well. The only constraint in this approach was pixel intensity. As the bone pixels have a clustered pattern, using the distance constraint can lead to better results. So in our new approach we imposed both the distance and intensity constraints. Thus, a multistage method based on vector quantization [8] is proposed for bone segmentation which has the following steps:

1. Feature Analysis of Image Data: The goal of the low-level processing is to classify the ROI voxels based on their local intensity vectors. It is reasonable to choose a local volume for each voxel, so we create a feature vector with 23 voxel intensity of its neighbors as shown in Fig 2 considering the partial volume effect and thickness of the voxels. To decrease the computing load, the principal component analysis (PCA) [9], [10] is then applied to the local vector series to determine the dimension of the feature vectors and the associated orthogonal transformation matrix [i.e., the Karhunen–Loeve (K–L) transformation matrix]. The PCA on the datasets of the training samples heuristically show that a rational dimension of the feature vectors is 5, where the summation of the first five principal components' variances is more than 92% of the total variance.

2. Vector Quantization Algorithm: For the low-level processing, in the K–L domain, the feature vectors are created by the first five principal components from the transformed vector series.

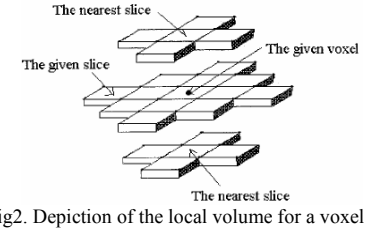

Fig2. Depiction of the local volume for a voxel [8].

Then, the feature vectors are classified into several classes with an automatic, unsupervised and self-adaptive vector quantization (VQ) algorithm.

The class number and the delegated vector for each class can be attained in a single scan on all feature vectors. The representative vector of each class is an estimation of the mean vector of that class. From the central limit theorem [11], the larger the number in a class is, the more accurate the representative vector estimates the mean vector of that class.

The number of classes and the representative vectors are updated continuously when more vectors are contained in the calculation. The updating process depends only on two parameters: the upper bound of possible classes (**K**) and the vector similarity threshold (**T**). In our MR data sets, there are roughly four classes that can be perceived based on their intensity features: 1) cartilage, 2) muscle, 3) bone, and 4) articular space where the intensity values increase from the lowest to the highest. In the available MR data sets, we want to segment the two bones: 1) acetabular and 2) femoral head that each one has a partial volume overlap to area soft tissue. Therefore, **K** is set to eight in this study. According to our numerical experiments, **T** is set to the square root of the maximum component variance of the feature vector series. The VQ algorithm is shown in fig 3.

3. Extraction of the bone: The results of the low-level classification are represented as a labeled image with integer values. The hip joint is composed of four kinds of labeled voxels: 1) acetabulum, 2) partial volume from acetabulum to soft tissue, 3) femoral head, and 4) partial volume from femoral head to soft tissue. By applying the inverse K–L transformation to the class representative vectors, the intensities in the original image space for each class are obtained.

3. Labeling the bones

In the result images we have the binarized femoral head and the acetabulum which have been segmented from the other structures. In order to segment the femoral head and acetabulum from each other, a circle with the same center obtained in Section *A* is fitted to each slices of the data set.

The extent of a femoral head is known in typical clinical cases of Hip joint [5]. Hence, a slice with an out of range radius was automatically disregarded in the operations. The largest 3D component connected to the estimated center inside the estimated circle is automatically segmented as the femoral head.

For segmenting the acetabulum in each slice, after excluding the femoral head from the whole binary data set, the largest and closest connected component corresponding to the femoral head upper boundary is segmented as acetabulum bone. All the operations mentioned above, are performed automatically. The procedure of segmenting the femoral head and acetabulum is shown in Fig 3. Fig 4 illustrates the supremacy of the vector quantization method in some slices which had inaccurate results in the previous method.

C. Segmentation of Hip Joint Space

We determined the outer edges of the femoral head and acetabulum in slice by slice manner and the extent of hip joint space is known in typical clinical cases. With these constraints, for each acetabular boundary point, we search for

the closest femoral boundary point. Concerning the maximum allowable size of a Hip joint gap that is fixed [4], a threshold is obtained. If the distance between the founded boundary points is less than the threshold obtained, the corresponding acetabular boundary point is kept; else it is excluded from the acetabular boundary.

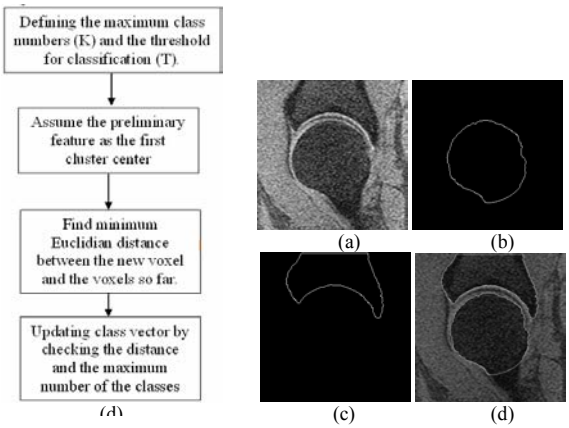

Fig. 3. The results of the clustering method on two slices of one data set.(a) The original image,(b) The segmented femur edge, (c) The segmented pelvis edge and (d) The overlaid edges with the original image. (d) The VQ algorithm.

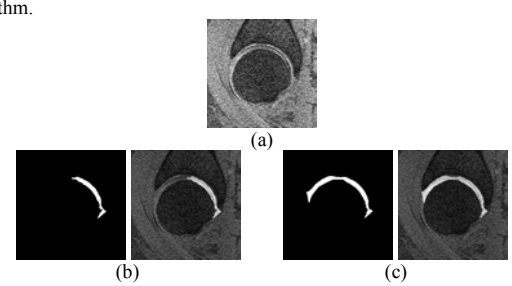

Fig. 4. Comparison of new approach with previous. (a) a typical slice that previous method failed. (b), (c) The result of previous and proposed methods and the overlay of them with the 4(a) and respectively.

The femoral head boundary points are determined in the same way by calculating the distance of each point on the boundary from the closest point in the acetabular boundary of the hip joint. By the threshold obtained in the previous paragraph, considered femoral boundary may be kept or excluded from the hip joint space boundary. The acetabular or femoral boundaries must have two points to the most in each row and column of image data. Thus, the two boundary points which are closest to all other boundary points are kept and extra boundary points are excluded from acetabular and femoral head boundaries. In the next step, we connect the corresponding heads and tails of acetabular and femoral head boundaries to perform the Hip joint space**.** The procedure of this step is illustrated in Fig5.

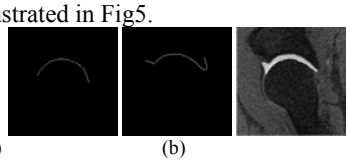

Fig.5. Segmentation of the joint space. (a,b) Resultant femoral and acetabulum boundaries in hip joint respectively, (c) the overlay of segmented hip joint with original image.

D. segmentation of the hip cartilages

In this step we use the segmented hip joint as the ROI to segment the cartilages. In our recent research we localized the articular space central line enhancing the images by developing a 3D directional derivative filters which were taken in radial direction from the center point of a sphere that approximated a femoral head. Then, we localize the articular space applying the canny edge detector filter to the enhanced images and impose anatomical constraint. To segmenting the hip cartilages we use morphological operations such as subtracting. We subtract the articular space from the segmented hip joint space.

III. RESULTS

The developed methods successfully applied to all the 20 sets of hip MR data. The datasets are grouped in three categories according to the contrast between the different tissues: 1-GOOD dataset, 2-MODERATE dataset and 3-POOR dataset where the GOOD dataset contains the images with the most obvious variations in the image intensity and the POOR dataset includes the images with the least obvious variations in the image intensity as showed in Fig 6. 6 sets of datasets were GOOD, 8 sets were MODERATE and the rest of them were POOR. The flowchart of the assessment showed in fig 7.

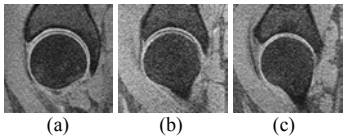

Fig6. Comparison of the data sets. (a) A typical GOOD, (b) MODERATE and (c) POOR data set

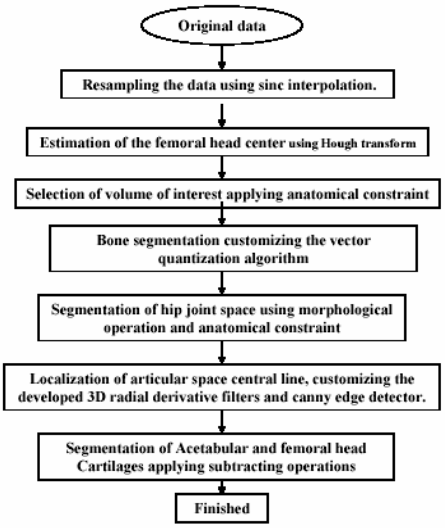

Fig. 7. The flowchart of the assessment.

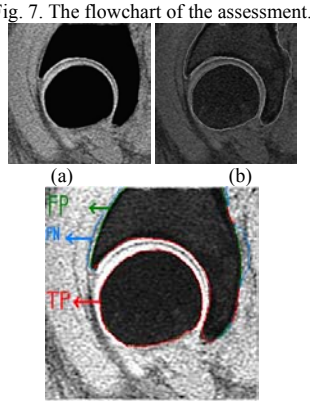

(c)

Fig. 8. (a) The manual segmentation of the bone, (b) The result of the SVD algorithm and (c) The overlay of (a) and (b) that showed the TP in red, FN in blue and FP in green.

To evaluate these two algorithms for segmenting the bones we compare them with the manual segmentations which had been segmented manually by the experts who were available at that time, in ROC diagrams. The success and failure of the algorithm is measured by finding the true positive rate (TPR) and false positive rate (FPR) in comparison with the previous method. In order to find the TPR we have to verdict the value of the true positive (TP) and the false negative (FN) and to define the FPR we have to decide the true negative (TN) and the false positive (FP). These values were corresponding to the four following types of tissues: (1) TP pixels (P_{TP}): correctly segmented bone tissues; (2) FP pixels (P_{FP}): non bone tissues recognized as bone tissues due to the failure of the technique; (3) FN pixels (P_{FN}) missed bone tissues; (4) TN pixels (P_{TN}): correctly did not segment as bone tissues. The examples of typical counting the FP, TP, FN and TN pixels are shown in Fig 8. The diagrams are shown in Fig 9. As can be seen in the diagrams the results of the proposed algorithm are in general better than the previous algorithm because the entire algorithm is done in 3D manner on the voxels. In this technique, segmenting the bone we have defined two constraints: a threshold for classification (**T**) and the maximum number of the classes (**K**). With these two constraints we consider the distance restriction and the image attribute. Accurate localization of the articular space central line is strong point that leads to better and more precision cartilage segmentation results. To draw the ROC curve for the proposed algorithm, T is changed from 0.1 to its optimum value mentioned in section *B* and for previous method we draw it by changing the filters window size from 3 to 15. The 3D volume of the segmented cartilage showed in Fig. 10.

IV. Conclusion

We have developed a fully automatic multi-step method for segmentation of hip joint bones and cartilages from MR images. In this study we used vector quantization algorithm for bone segmentation. We customized an accurate segmentation of the articular space from our recent research to segment the hip cartilages.

In the presence of available data sets, the results were promising. We quantify the new method in ROC diagrams in comparison with the previous segmentation technique.

We need to evaluate the algorithms with more data sets, integrate the proposed technique in a software package for cartilage segmentation and to cartilage thickness map estimation and the corresponding 3D visualizations.

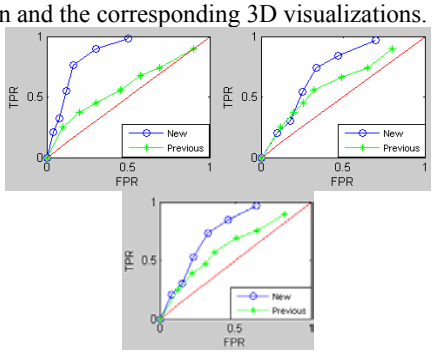

Fig. 9. The ROC curve to compare two methods illustrated in section B. The blue curves correspond to the clustering method and green curves show the result of thresholding method in (a) GOOD (b) MODETARE (c) POOR (d) ALL datasets. The red line is x=y.

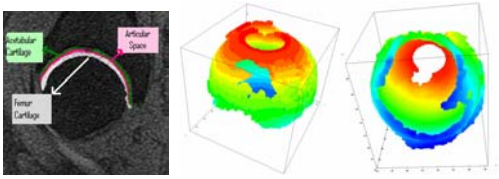

(a) (b)

Fig. 10. The segmented cartilages of the Hip joint. (a) Segmented cartilages in one slice. (b) Two views of 3D rendering of the sick hip joint cartilages. The hole common in the pictures is because of the ligament that reinforces the femoral head in its place. The color assigned for better perception of the depth.

References

[1] T. Nishii, K. Nakanishi, N. Sugano, K. Masuhara, K. Ohzono and T. Ochi, "Articular cartilage evaluation in osteoarthritis of the hip with MR imaging under continuous leg traction" *Magnetic Resonance Imaging*. Vol. 16, No. 8, pp. 871-875, 1998.

[2] PR Kornaat, SB Reeder, S. Koo et al., "MR imaging of articular cartilage at 1.5 T and 3.0 T: Comparison of SPGR and SSFP sequences", *OsteoArthritis and Cartilage*, Vol. 13, pp. 338-344, 2005.

[3] R. A. Zoroofi, Y. Sato, T. Nishii, K. Nakanishi, H. Tanaka, N. Sugano, H. Yoshikawa, H. Nakamura and Sh. Tamura, "Automated Segmentation of Acetabular Cartilage in MR images of the Hip" *Proceedings of the CARS Conference*, 2005.

[4] T. Nishii, N. Sugano, Y. Sato et al., "Three-dimensional distribution of acetabular cartilage thickness in patients with hip dysplasia: a fully automated computational analysis of MR imaging", OsteoArthritis and Cartilage, Vol. 12, pp. 650-657, 2004.

[5] M. Khanmohammadi, R. A. Zoroofi, Y. Sato, T. Nishii, K. Nakanishi, H. Tanaka, N. Sugano, H. Yoshikawa, H. Nakamura, S. Tamura, "Automated Segmentation of the Articular Space in MR Images of the Hip Joint", *In Press,*2006.

[6] Y. Sato, K Nakanishi, H Tanaka et al., "A fully automated method for segmentation and thickness determination of hip joint cartilage from 3D MR data", *Proc. CARS: International Congress Series*, Vol. 1230, pp. 352–358, 2001.

[7] N Otsu, "A Threshold Selection Method from Gray Level Histograms", *IEEE Trans. Systems, Man and Cybernetics*, Vol. 9, pp: 62-66, 1979.

[8] D. Chen, Z. Liang, M. R.Wax, L. Li, Bin Li, and A. E. Kaufman. "A Novel Approach to Extract Colon Lumen from CT Images for Virtual Colonoscopy" *IEEE Trans. Medical Imaging*, Vol. 19, pp. 1220-1226, No. 12, 2000.

[9] K. Fukunaga, *Introduction to Statistical Pattern Recognition*, 2nd ed. New York: Academic, 1990.

[10] C. Chatfield and A. J. Collins, *Introduction to Multivariate Analysis*. London, U.K.: Chapman & Hall, 1980.

[11] W. Feller, An Introduction to Probability Theory and its Applications, 3rd ed. New York: Wiley, 1968.